OPEN EUROPEAN JOURNAL ON VARIABLE STARS
October 2009 http://var.astro.cz/oejv ISSN 1801–5964

# LIGHT CURVE ANALYSIS OF XX CYGNI FROM DATA TAKEN USING DSLR

Fiacconi, Davide[1]; Tinelli, Luciano[2]

1) Carnate (MB), Italy, Gruppo Astrofili Villasanta, davide.fiacconi@gmail.com
2) Usmate-Velate (MB), Italy, Gruppo Astrofili Villasanta, luciano.tinelli@fastwebnet.it

**Abstract:** XX Cygni belongs to the SX Phoenicis class of short period variable stars. The pourpose of this paper is to analize data taken by the authors with a common Digital Single Lens Reflex (DSLR) and try to understand the capability of this type of camera in photometric measurements. From data taken during summertime and from the AAVSO International Database, we try to determine the behaviour of the main period of the star and research for other important frequency component by periodigram and Observed-Calculated (O-C) diagram.

XX Cyg ($20^h$:$03^m$:$15.6^s$;+58°:57′:17.0″) belongs to the SX Phoenicis class of short period variable stars. It is located in Cygnus, near the boundary between Draco and Cepheo, and it owes its brightness variation to pulsation processes in the external shells.

## 1 Images acquisition and reduction

Images were all taken using a 80 mm diameter apochromatic refractor ($f/7$) with a Canon EOS 400D DSLR camera, from Usmate-Velate[1]: they were all acquired in RAW format at 800 equivalent ISO, with 60-80 s time exposure, depending on sky condition. It was first estimated the linearity interval of the camera following Nicolini[2]. This camera is equipped with a color CMOS sensor the pixel of which are covered by a matrix of coloured filters (the so called Bayer matrix), respectively green (G1), red (R), blue (B) and green (G2). Images were also slightly defocused to increase the surface interested by stellar flux. The main features of the imaging sessions are resumed in Table 1. We also decided to use a data set from the A.A.V.S.O.[3] International Database obtained with astronomical CCD and V filter. It definitely improves the following analysis because of the quality of the datas and because measurements are note in phase with ours. In total we considered 1003 DSLR and 197 CCD observations.

Regarding image reduction, we decided to use the Iris[4] package. We debayerized our frames with debayerized offsets, dark subtraction and flat normalization. We then split every frame in four images composed by the G1, R, B and G2 pixels. From the two sets of G images, we measured variable and references star fluxes with the utility *Automatic Photometry*. In this way, we obtained two values for the fluxes in the G channel and magnitude differences, $\Delta m$, were calculated as difference between the variable star magnitude and the magnitude of the sum of the reference stars. In Table 2 stars used as references are listed.

[1]Usmate-Velate (MB), Italia, lat: 45° 35’ 33” N, long: +9° 21’ 33” E, alt: ≈ 250 m
[2]Nicolini, G., 2008, http://astronomiadigitale.blogspot.com/
[3]American Association of Variable Star Observers, http://www.aavso.org/
[4]IRIS by Christian Buil: http://www.astrosurf.com/buil/us/iris/iris.htm

| # | Date (HJD) | Time Interval (HJD) | N° of images | $\Delta t_p$ (min) |
|---|---|---|---|---|
| 1* | 2455011 | +0.6153539 – +0.8447395 | 197 | 2 – 3 |
| 2 | 2455029 | +0.4083565 – +0.5422569 | 109 | 1 – 2 |
| 3 | 2455035 | +0.4181944 – +0.5318866 | 93 | 1 – 3 |
| 4 | 2455048 | +0.3436227 – +0.5373842 | 126 | 1 – 2 |
| 5 | 2455050 | +0.3272106 – +0.4349421 | 122 | 1 – 2 |
| 6 | 2455055 | +0.3392129 – +0.4237500 | 89 | 1 – 2 |
| 7 | 2455062 | +0.3251273 – +0.4394097 | 87 | 1 – 2 |
| 8 | 2455071 | +0.3308466 – +0.5889884 | 203 | 1 – 2 |
| 9 | 2455074 | +0.3528695 – +0.5563966 | 174 | 1 – 2 |
| ** - Datas from A.A.V.S.O. International Database* | | | | |

Table 1: Summary of the imaging sessions. Columns are heliocentric Julian day based on UTC (HJD), time interval covered during the night (HJD), number of shoots for session and rest times between consecutive images.

| Stella | RA | Dec | Magnitudine (V) |
|---|---|---|---|
| GSC 03948-01025 | 20h 09m 02.70s | +58° 19' 05.7" | $8.425 \pm 0.014$ |
| GSC 03944-00281 | 20h 05m 30.19s | +57° 59' 53.5" | $9.208 \pm 0.019$ |
| GSC 03944-00674 | 20h 04m 19.14s | +58° 00' 39.2" | $9.582 \pm 0.023$ |

Table 2: Stars used as references. Magnitudes are taken from Tycho-2 catalogue.

## 2 Results

Fourier analysis is fundamental to understand the presence of different frequencies in a periodic signal. First of all, we transformed the original geocentric Julian dates to heliocentric Julian dates based on UTC (HJD) and we normalized the whole data set to get:

$$\sum_j \Delta m_j = 0.$$

### 2.1 Periodigram analysis

Astronomical data can be well investigated with the algorithm proposed by Ferraz-Mello (1981), the Date Compensed Dicrete Fourier Transform, which allows one to analyse unevenly spaced data. A C++ tool was written to compute the DCDFT periodigram and the result of the elaboration was plotted using the ROOT[5] package in Figure 1, together with the spectral window produced using the Period04[6] package. It is clearly visible a principal frequency, at the value, obtained by interpolation, of:

$$\nu_{princ} = 7.41464 \quad c\ d^{-1}, \tag{1}$$

where $c\ d^{-1}$ is the number of cycles per day.

Finally, we generated a Monte Carlo simulation to determine the error values for the main frequency $\nu_{princ}$. New data sets were made from the original one through Gaussian

[5]ROOT, a data analysis framework, http://root.cern.ch/drupal/
[6]Period04, http://www.univie.ac.at/tops/Period04/

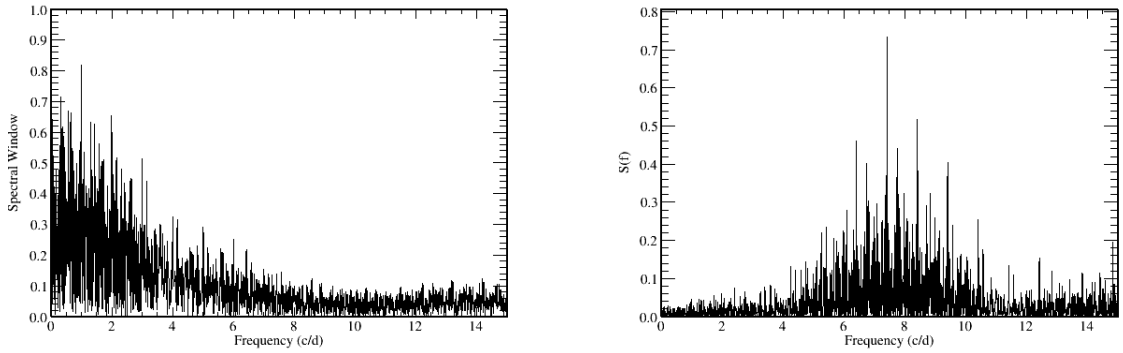


Figure 1: The picture on the left shows the spectral window, while that on the right the DCDFT periodigram, obtained with $d\nu = 0.001$. It is possible to see clearly, in the periodigram, the principal frequency.

smearing of the $\Delta m$ values and using their errors as variance for the Gaussian distributions. Then, every new set was analysed by DCDFT periodigram to obtain new simulated frequency measurements. The distribution of the simulated frequencies is shown in Figure 2, based on one thousand iterations. A Gaussian function was used to calculate the

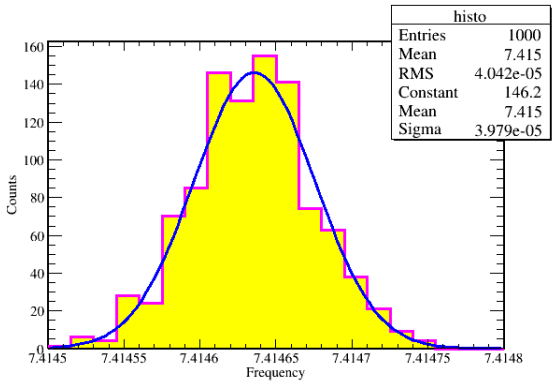


Figure 2: The bar chart shows the distribution of the frequencies obtained from one thousand iterations derived by a Monte Carlo simulation. A Gaussian fit is applied to calculate the standard deviation of the distribution.

standard deviation of the distribution:

$$\sigma_\nu = 3.97883 \times 10^{-5} \quad c\ d^{-1}. \tag{2}$$

Therefore, we can conclude that the measure of the main pulsation period of XX Cygni is:

$$\nu_{princ} = 7.41464 \pm 0.00004 \quad c\ d^{-1}, \tag{3}$$

with relative period:

$$T_{princ} = 0.1348683 \pm 0.0000007 \quad d. \tag{4}$$

It is possible to compare this value with $T = 0.1348652 \pm 0.0000001\ d$, as reported in Zhou et al. (2002). The value obtained by us seems to be in fairly good agreement with it. the whole data set and the phase diagram obtained using $T_{princ}$ are shown in Figure 3.

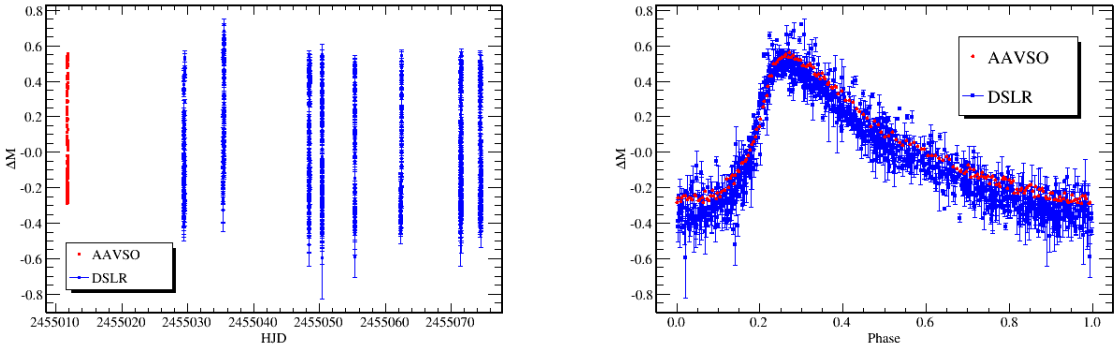


Figure 3: In the left plot the whole data set is shown. In the right the phase diagram obtained with $T_{princ}$ is also shown. A.A.V.S.O. data are highlighted.

## 2.2 Light curve analysis

From what we had previously measured , we analised the light curve by Fourier expansion. We used a generic expansion with the sin terms as:

$$I(t) = a_0 + \sum_{n=1}^{+\infty} a_n \sin\left(2\pi\nu n\ t + \varphi_n\right), \tag{5}$$

and we applied least square methods to calculate parameters $a_n$ and $\varphi_n$ for a particular frequency. First of all, we studied the whole data set to understand what harmonics result more significant. We derived that all the harmonics beyond the tenth are completely negligible and mingles with the ground noise, again in agreement with Zhou et al. (2002). Figure 4 showes the DFT of the data set after having removed the first nine harmonics. We also plotted the distribution of the residuals (Figure 5) which is Gaussian. We also

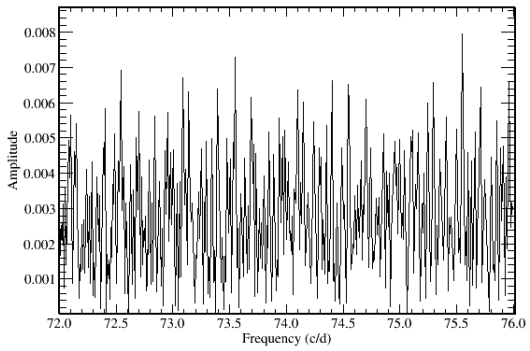


Figure 4: It is shown the DFT of the data set after it was filtered by the first nine harmonics. It is possible to see that 10 $\nu_{prin} = 74.1464\ c\ d^{-1}$ is not distinguishable from the ground noise.

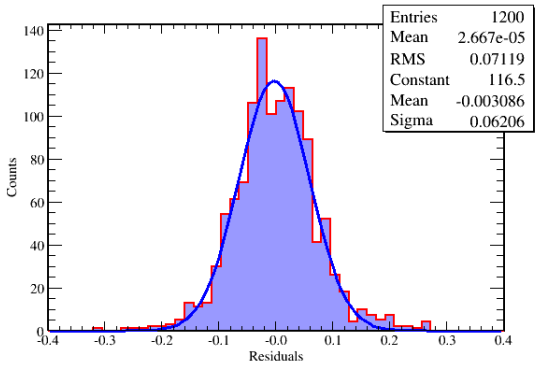


Figure 5: Ditribution of the residuals obtained from the difference between original datas and Fourer expansion fit based on $\nu_{princ}$ and its harmonics. A gaussian fit is superimposed.

used the Fourier expansion to determine the main pulsation frequency. The results of the fit are reported in Table 3 with the respective errors, which were calculated by a Monte Carlo simulation of one thousand iterations. After the optimization, the average value of

| # | $\nu$ (c/d) | $\sigma_\nu$ (c/d) | $a_n$ (mag) | $\sigma_{a_n}$ (mag) | $\varphi_n$ (rad) | $\sigma_{\varphi_n}$ (rad) |
|---|---|---|---|---|---|---|
| 1 | 7.414677 | 0.000062 | 0.340231 | 0.003881 | 0.384337 | 0.001437 |
| 2 | 14.829492 | 0.000153 | 0.144362 | 0.003525 | 0.227357 | 0.003933 |
| 3 | 22.244604 | 0.308602 | 0.082974 | 0.020470 | 0.339765 | 0.121422 |
| 4 | 29.659203 | 0.499617 | 0.044490 | 0.011983 | 0.142693 | 0.139752 |
| 5 | 37.075138 | 0.366079 | 0.027720 | 0.008291 | 0.627779 | 0.171461 |
| 6 | 44.489155 | 0.001238 | 0.020259 | 0.003428 | 0.126728 | 0.031786 |
| 7 | 51.904962 | 0.001630 | 0.015796 | 0.003006 | 0.329822 | 0.035832 |
| 8 | 59.319403 | 1.015230 | 0.009613 | 0.003570 | 0.784051 | 0.128657 |
| 9 | 66.733745 | 0.424773 | 0.007950 | 0.002768 | 0.992418 | 0.192399 |

Table 3: In table are reported the results of the fit after the optimization of all the parameter values. Uncertainties are obtained with a Monte Carlo simulation of one thousand iterations.

the residuals decreased from 0.0711 to 0.0705 and the new main pulsation frequency is slightly different from the one calculated by periodigram:

$$\nu_{fit} = 7.414677 \pm 0.000062 \quad c\ d^{-1}, \tag{6}$$

with the period:

$$T_{fit} = 0.1348676 \pm 0.0000011 \quad d. \tag{7}$$

The two value are however in agreement within the errors. Moreover, other important frequencies were not found.

## 3 O-C diagram analysis

It is always usefull to make reference to an O-C diagram to research for long time behaviour of the pulsation period. During our imaging sessions (except for $n\#$ 2) we always observed one or two maxima. After the heliocentric correction, we measured the time of each maximum by means of an interpolation with a $5^{th}$ degree polynomial. The measured values are shown in Table 4. We joined our data with the collection of times of maximum reported in Blake et al. (2002) to improve the analysis (we rejected four values which were clear outliers). All times of maximum were calculated using the ephemerides in Kiss & Derekas (2000), as reported in Szeidl & Mahdi (1981):

$$HJD_{max} = 2430671.1010 + 0.134865070 \times E. \tag{8}$$

In Figure 6, the O-C diagram is shown with superimposed the quadratic fit. The mean uncertainty on the measurements is $\sigma_{O-C} \approx 0.0015$. We got $\chi^2/ndf = 137.1/122$, with probability $P \approx 0.17$. The quadratic fit is due to the hypothesis of a linear behaviour for the period, as confirmed in Figure 7, which shows the residuals after that the fit was subtracted, and their Gaussian distribution. It is possible to see qualitatively that our data follow a trend consistent with the one defined by historical data. In particular, from the fit we derive:

$$O - C = 1.56 \times 10^{-3}(23) + 4 \times 10^{-9}(3)\ E + 2.82 \times 10^{-13}(23)\ E^2. \tag{9}$$

From the last expression we can obtain new ephemerides:

$$HJD_{max} = 2430671.10256(23) + 0.134865074(3)\ E + 2.82 \times 10^{-13}(23)\ E^2. \tag{10}$$

| O max (1) | C max (2) | E (3) | O-C (4) |
|---|---|---|---|
| 2455011.694 | 2455011.684 | 180481 | 0.010 |
| 2455011.830 | 2455011.819 | 180482 | 0.011 |
| 2455035.432 | 2455035.420 | 180657 | 0.012 |
| 2455048.379 | 2455048.367 | 180753 | 0.012 |
| 2455048.514 | 2455048.502 | 180754 | 0.012 |
| 2455050.399 | 2455050.390 | 180768 | 0.009 |
| 2455055.393 | 2455055.380 | 180805 | 0.013 |
| 2455062.403 | 2455062.393 | 180857 | 0.010 |
| 2455071.442 | 2455071.429 | 180924 | 0.013 |
| 2455071.575 | 2455071.564 | 180925 | 0.011 |
| 2455074.408 | 2455074.396 | 180946 | 0.012 |
| 2455074.542 | 2455074.531 | 180947 | 0.011 |

Table 4: In table are reported the observed times of maximum (1), the calculated times of maximum from equation 8 (2), the cycles number E (3) and the difference between observed and calculated time of maximum (4).

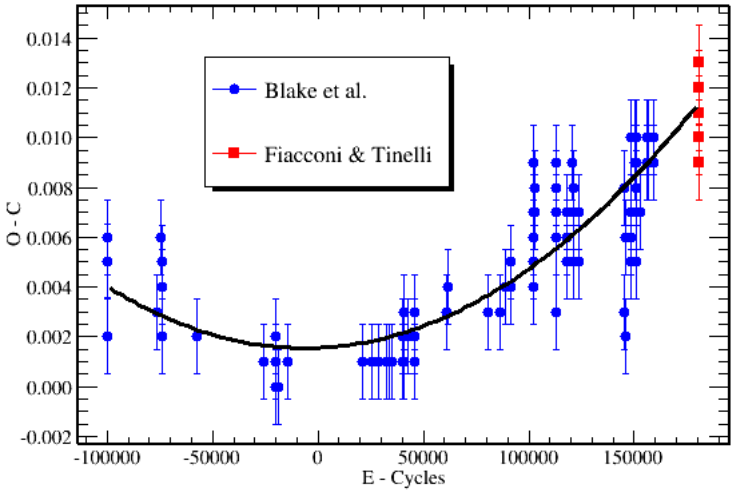


Figure 6: In the figure is shown the O-C diagram with superimposed the quadratic fit. Blu points are from Blake et al. (2002), red points are from our measurements.

About the fit, the quadratic coefficient is very important because it is linked with the period change in time. Although the period varies with continuity in time, in practice we measure it cycle by cycle, that is with the discrete variable $E$. In general, we have, for the times of maximum:

$$T_E^{(m)} = T_0 + \sum_{n=0}^{E} P_n. \tag{11}$$

For $P_n$ we assume that $P$ depends on the cycle number $n$: if the dependence is linear, the period will be:

$$P_n = P_0 + \delta P \; n, \tag{12}$$

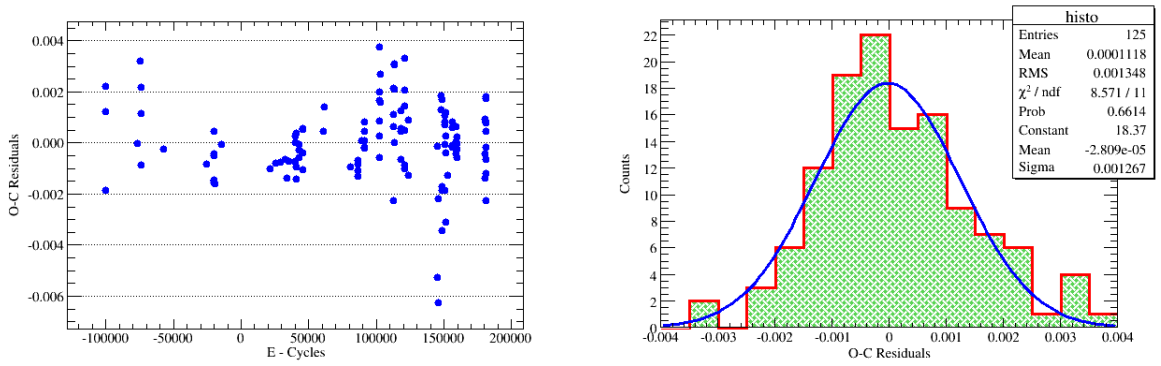


Figure 7: In the left hand figure residuals after the quadratic fit was subtracted are shown. It is possible to see that they mostly fall near the 0 line. In the right hand figure the distribution of the residuals with superimposed the Gaussian fit is shown.

where $\delta P$ is the discrete period increase from cycle to cycle, that we supposed to be constant due to the linear dependence. From equations 11 and 12 we obtain:

$$T^{(m)} = T_0 + \bar{P}E + \frac{1}{2}\delta P E^2, \tag{13}$$

where $E$ is the generic cycle number and:

$$\bar{P} = P_0 + \frac{1}{2}\delta P E = P_0 + \frac{\Delta P}{2}, \tag{14}$$

is the average period. That being so, we can assert that the star shows a period change:

$$\delta P = [5.64 \pm 0.46] \times 10^{-13} \quad d\ c^{-1}, \tag{15}$$

which is in fairly good agreement with the value suggested by Blake et al. (2002), that is $[5.64 \pm 0.12] \times 10^{-13}\ d\ c^{-1}$. It is also of the same order of magnitude with $4.84 \times 10^{-13}\ d\ c^{-1}$, reported by Zhou et al. (2002). We can also obtain the relative variation on the average period:

$$\frac{\delta P}{\bar{P}} = [4.18 \pm 0.34] \times 10^{-12}, \tag{16}$$

and the relative variation on the whole time interval (our and historical measurements):

$$\frac{\Delta P}{\bar{P}} = [1.19 \pm 0.46] \times 10^{-7}. \tag{17}$$

which is slightly larger than the values reported in Zhou et al. (2002) and Szeidl & Mahdi (1981), respectively $12.6 \times 10^{-8}$ and $8.7 \times 10^{-8}$. It is of the same order of magnitude with $6.9 \times 10^{-7}$ (Kiss & Derekas, 2000).

## 4 Conclusions

In this paper, the light curve and the O-C diagram of XX Cygni was analysed obtaining information about the behaviour of the pulsation period. The presented results are relevants from two points of view: 1) they improve the knowledge of variability parameters for this star; 2) they are obtained using a commercial DSLR.

From data taken during different imaging sessions, the periodigram analysis and the Fourier expansion of the light curve allow us to estimate the pulsation period:

$$T = 0.1348683 \pm 0.0000007 \quad d.$$

Moreover, frequencies till the ninth harmonic assume high significance in the light curve. It suggestes that transient processes with short period are present in the star and probably they are the cause of bumps in the descending arm of the curve, as shown in Blake et al. (2002). Multiperiodicity were not indentified.

We also used our 12 times of maximum to update measurement presented in Blake et al. (2002). New ephemerides were computed:

$$HJD_{max} = 2430671.10256 + 0.134865074\ E + 2.82 \times 10^{-13}\ E^2,$$

and we also found that the period change in XX Cygni is:

$$\delta P = [5.64 \pm 0.46] \times 10^{-13} \quad d\ c^{-1}.$$

In conclusion, it is possible to state that our results are fully consistent with what previously published in literature. Taking again into account that all our data were obtained with a common digital camera, this seems to indicate that DSLR could be used for homogeneous observation campaign of differential photometry with fairly good results.

**Aknowledgements:** We acknowledge with thanks the variable star observations from the A.A.V.S.O. International Database contributed by observers worldwide and used in this research. We also acknowledge with thanks Stefano Covino (INAF) for his help and precious advices to improve the quality of this paper.

## References

Blake, R. M., Delaney, P., Khosravani, H., Tome, J., Lightman, M., 2002, *Publ. Astron. Soc. Pacific*, **115**, 212-217, 2003PASP..115..212B

Ferraz-Mello, S., 1981, *AJ*, **86**, 619-624, 1981AJ.....86..619F

Kiss, L. L., Derekas, A., 2000, *Inf. Bull. Variable Stars*, **4950**, 1-4, 2000IBVS.4950....1K

Szeidl, B., Mahdi, H. A., 1981, *Comm. Konkoly Obs.*, $N^o$ 75, 1-35, 1981CoKon..75....1S

Zhou, A.-Y., Jiang, S.-Y., Chayan, B., Du, B.-T., 2002, *Astrophysics and Space Science*, **281**, 699-714, 2002Ap&SS.281..699Z